Supplementary Materials: Structures and Properties of Dinitrosyl Iron and Cobalt Complexes Ligated by Bis(3,5-diisopropyl-1-pyrazolyl)methane

Haruka Kurihara, Ayuri Ohta and Kiyoshi Fujisawa

Contents

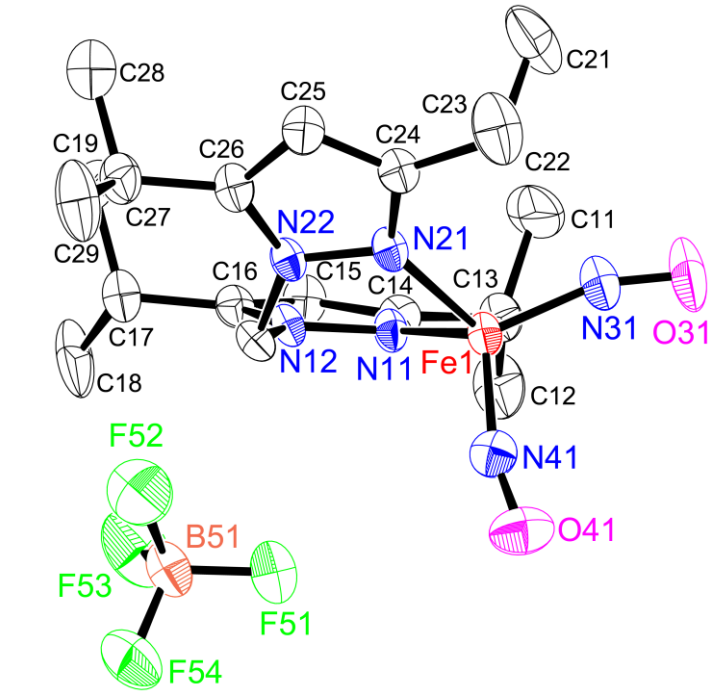

Figure S1. Crystal structure of $[Fe(NO)_2(L1'')](BF_4)$.

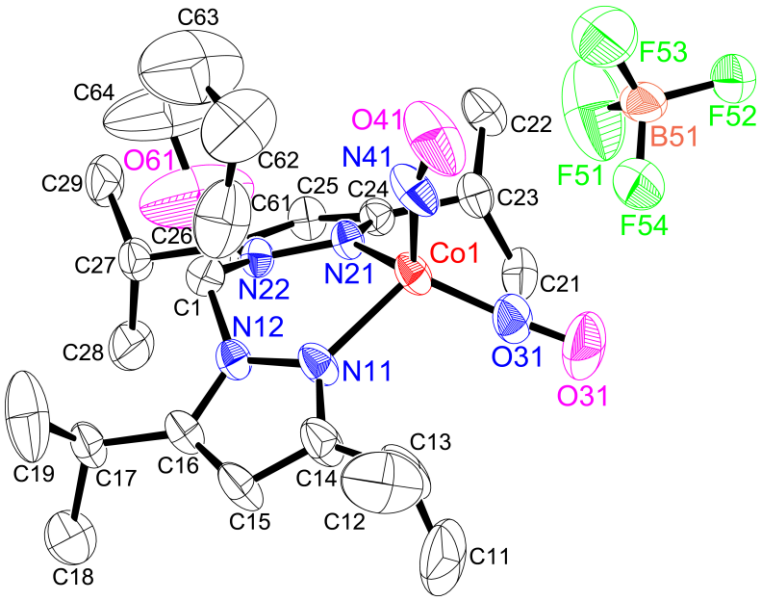

Figure S2. Crystal structure of $[Co(NO)_2(L1'')](BF_4)\cdot thf$.

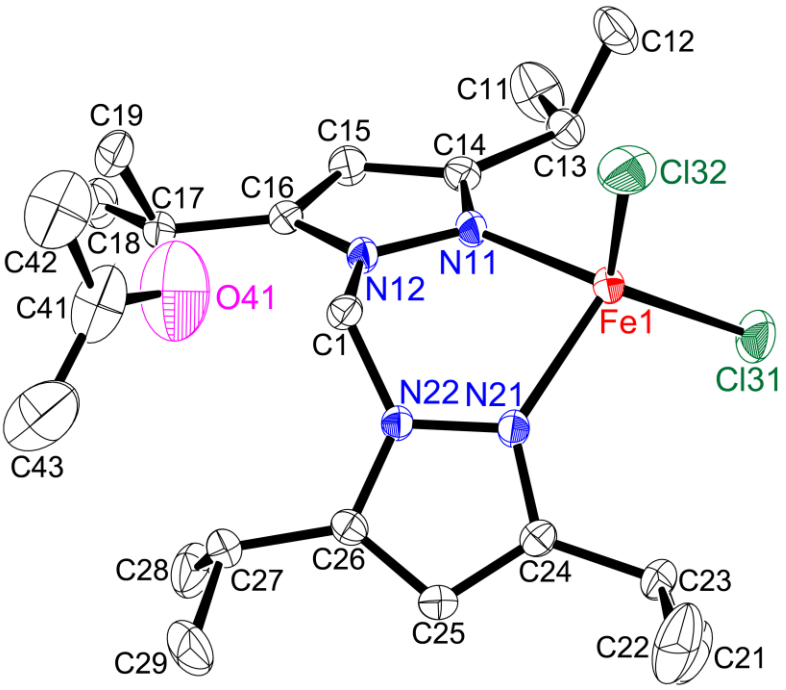

Figure S3. Crystal structure of $[FeCl_2(L1'')]\cdot(CH_3)_2CO$.

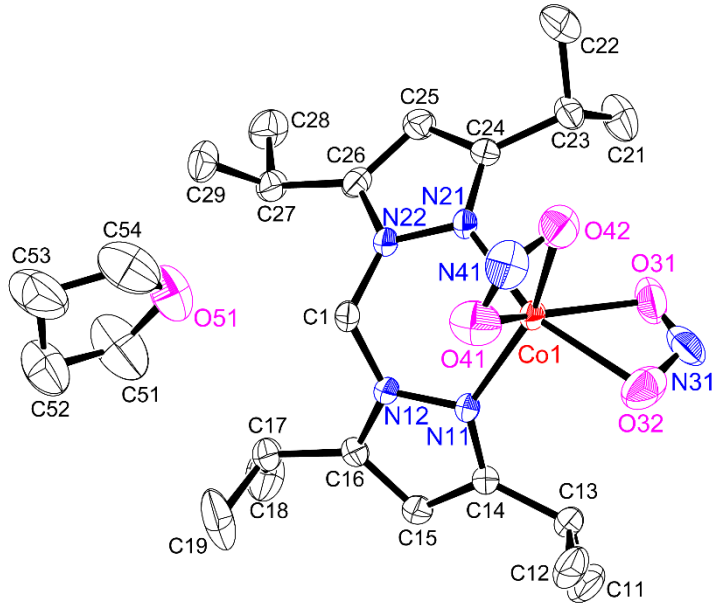

Figure S4. Crystal structure of $[Co(NO_2)_2(L1'')]\cdot thf$.

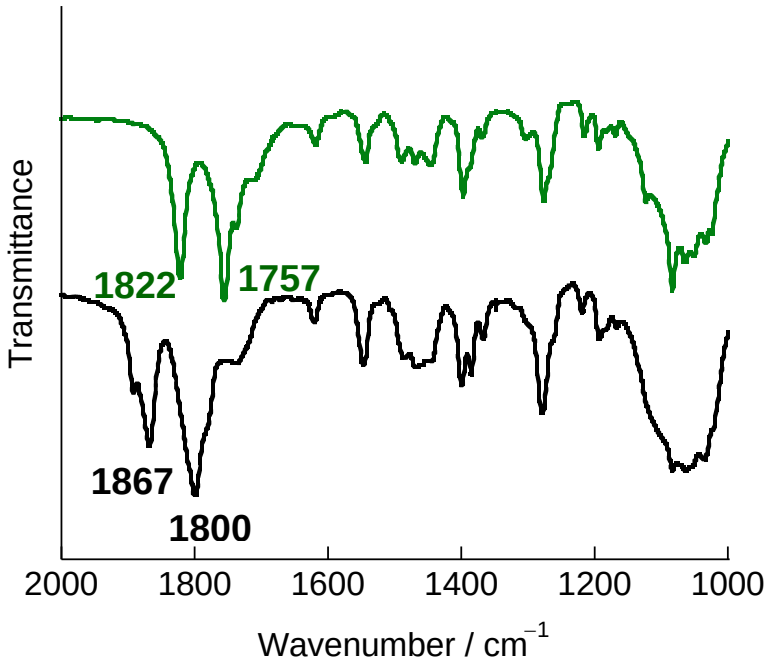

Figure S5. IR spectra of [Fe(NO)$_2$(L1")](BF$_4$) (green, top) and [Co(NO)$_2$(L1")](BF$_4$) (black, bottom) in the solid state (KBr).

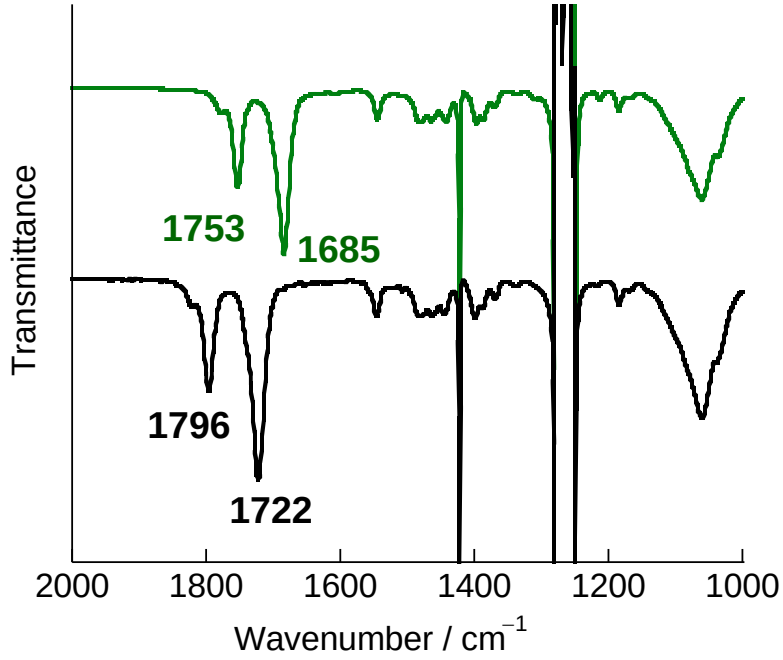

Figure S6. IR spectra of [Fe(^{15}N^{18}O)$_2$(L1")](BF$_4$) (green, top) and [Co(^{15}N^{18}O)$_2$(L1")](BF$_4$) (black, bottom) in solution (CH_2Cl_2).

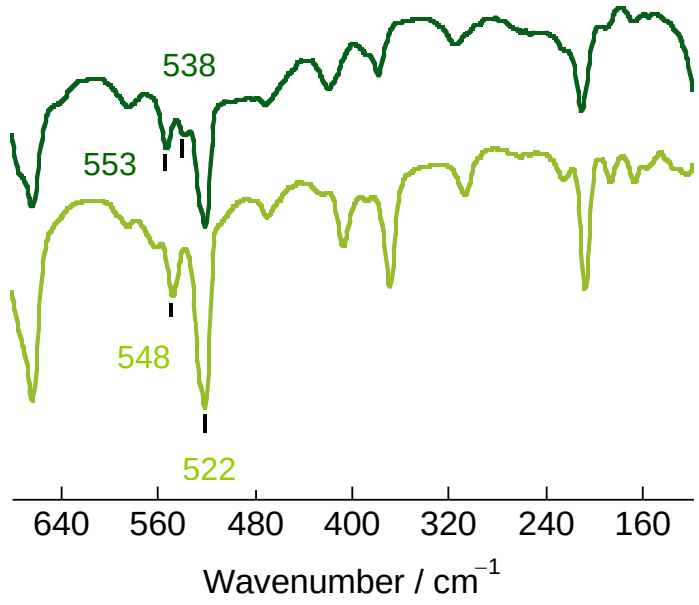

Figure S7. Far-IR spectra of $[Fe(NO)_2(L1'')](BF_4)$ (top, deep green) and $[Fe(^{15}N^{18}O)_2(L1'')](BF_4)$ (bottom, yellow green).

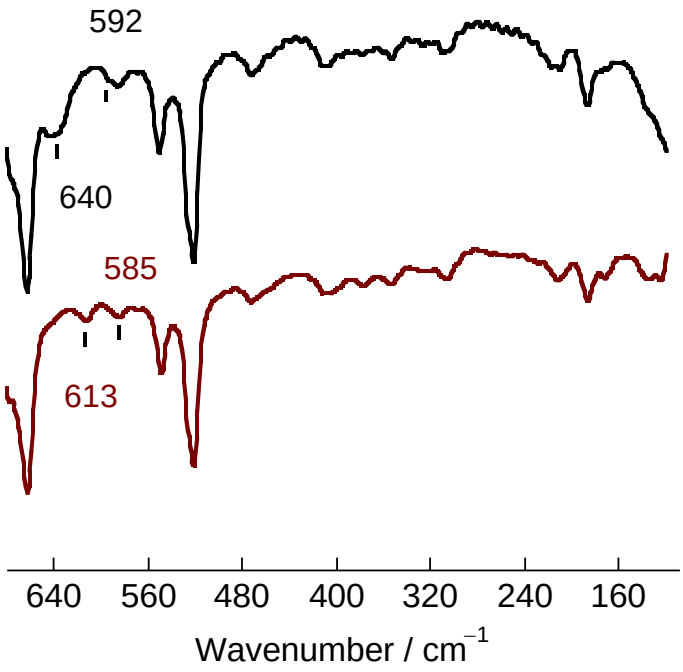

Figure S8. Far-IR spectra of $[Co(NO)_2(L1'')](BF_4)$ (top, black) and $[Co(^{15}N^{18}O)_2(L1'')](BF_4)$ (bottom, brown).

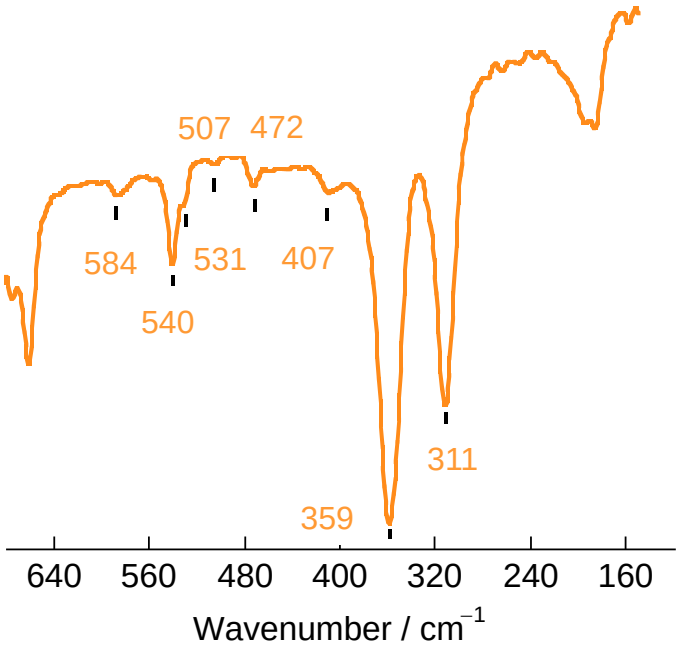

Figure S9. Far-IR spectra of $[FeCl_2(L1'')](BF_4)$ (CsI pellet).

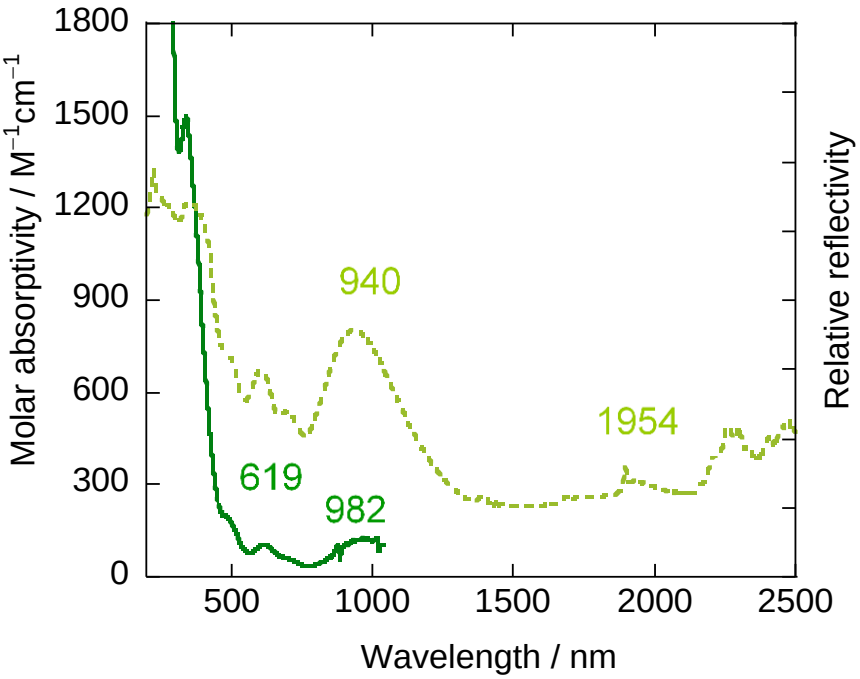

Figure S10. UV-vis (solid line, in CH_2Cl_2) and diffuse reflectance (dotted line, solid) spectra of $[Fe(NO)_2(L1'')](BF_4)$.

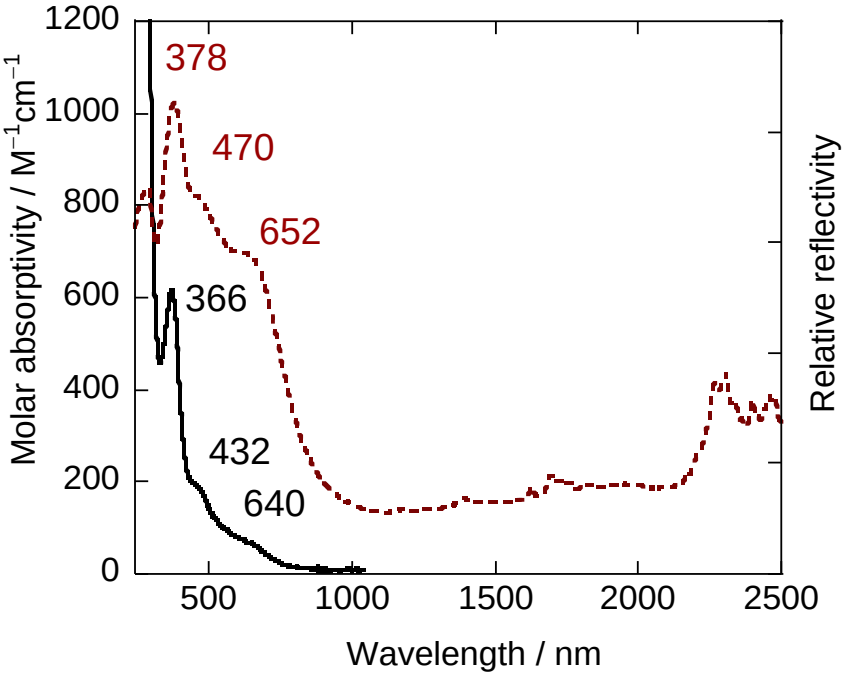

Figure S11. UV-vis (solid line, in CH_2Cl_2) and diffuse reflectance (dotted line) spectra of $[Co(NO)_2(L1'')](BF_4)$.

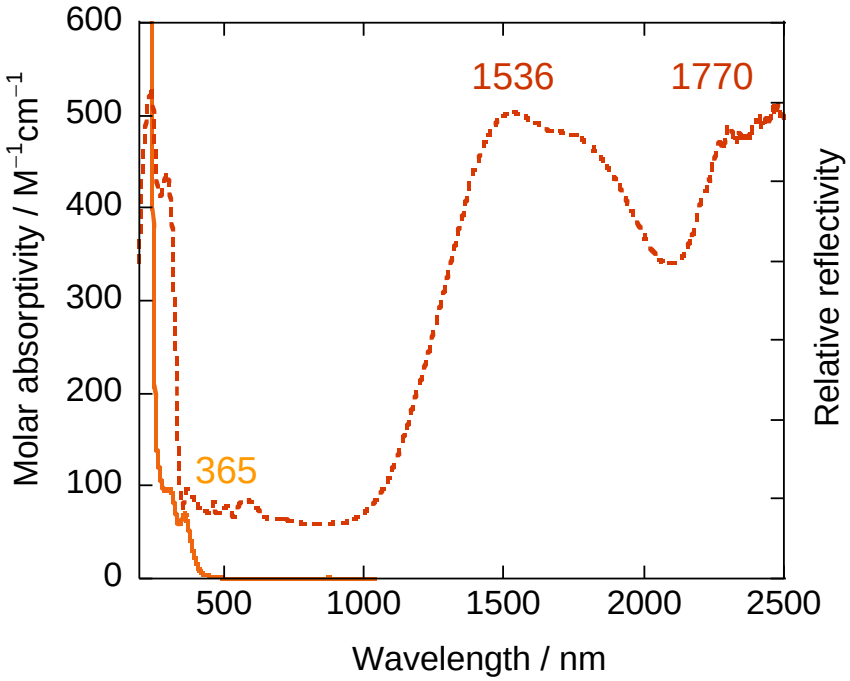

Figure S12. UV-vis (solid line, in CH_2Cl_2) and diffuse reflectance (dotted line) spectra of $[FeCl_2(L1'')]$.

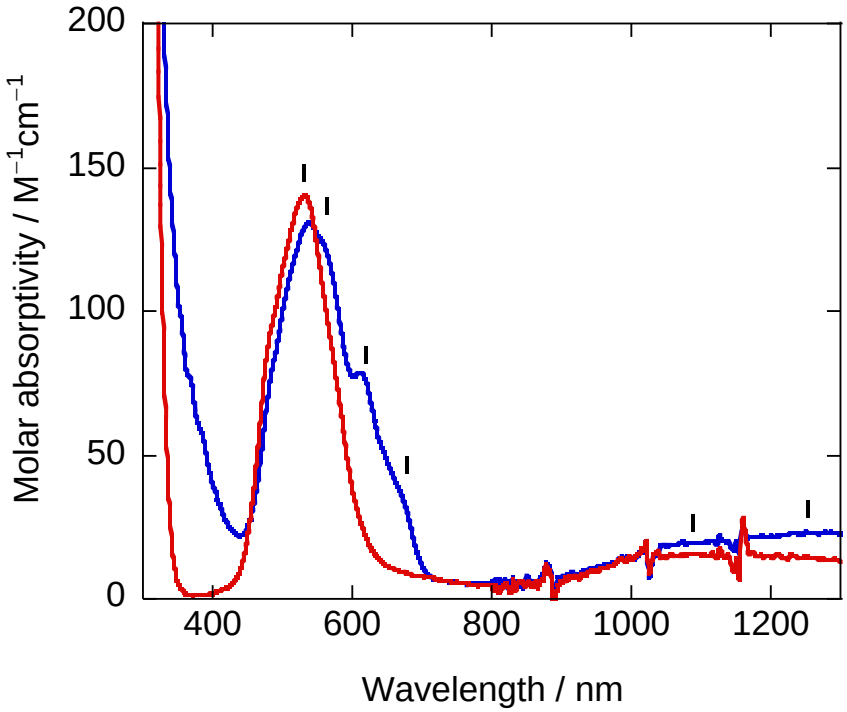

Figure S13. UV-vis spectra of [Co(κ^2-$O_2NO)_2$(L1")] (red) and [Co(κ^2-$O_2N)_2$(L1")] (blue) in CH_2Cl_2.

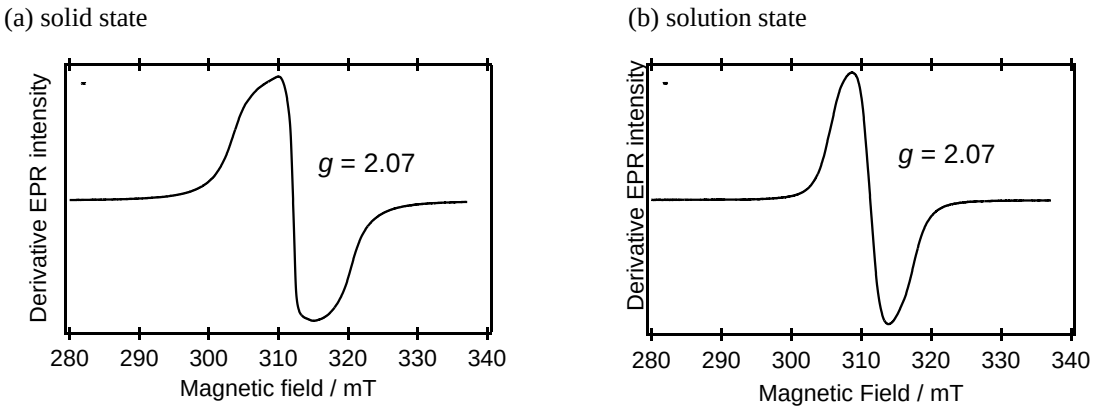

Figure S14. EPR spectra of [$Fe(NO)_2$(L1")](BF_4) in solid (left) and frozen dichloromethane solution (right) at 130 K.

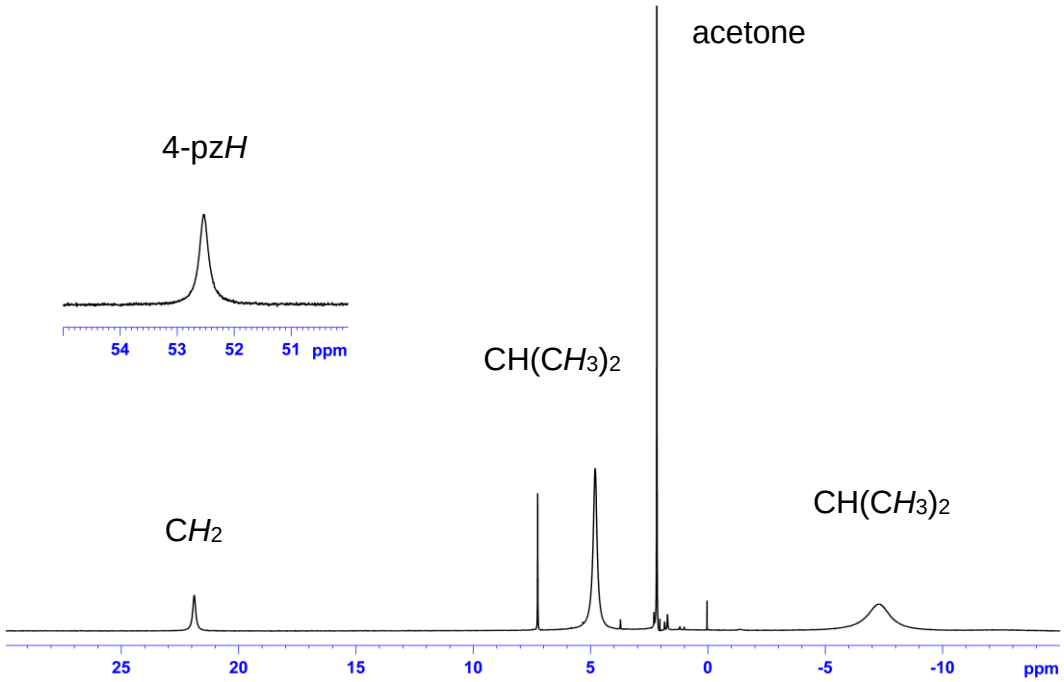

Figure S15. ^{1}H-NMR spectrum of [$FeCl_2$(L1")] in $CDCl_3$ at room temperature.

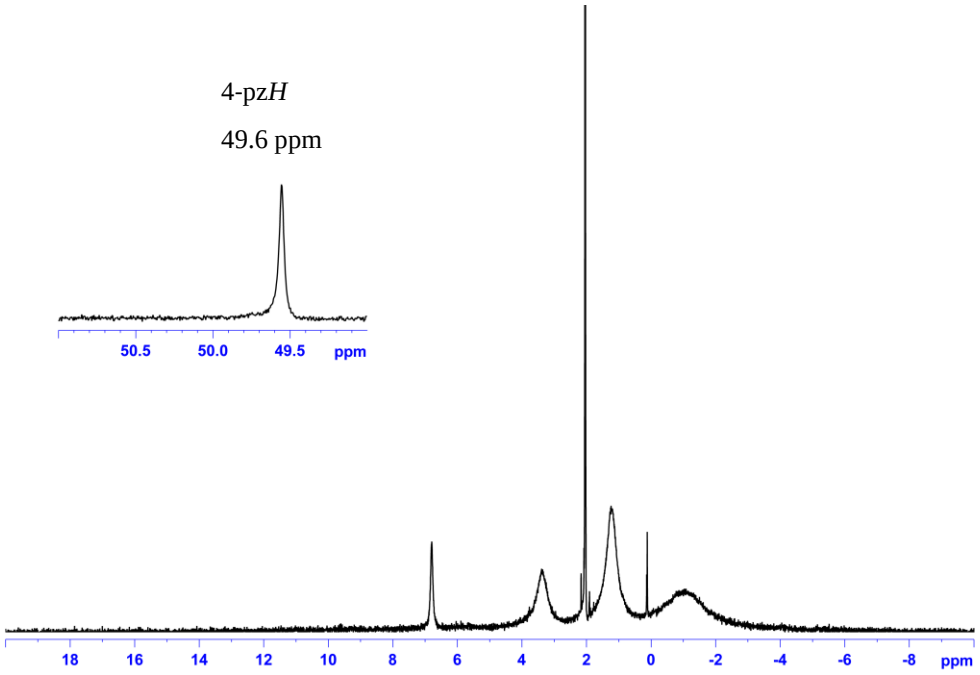

Figure S16. ^{1}H-NMR spectrum of [Co(κ^2-$O_2NO)_2$(L1")] in $(CD_3)_2CO$ at room temperature.

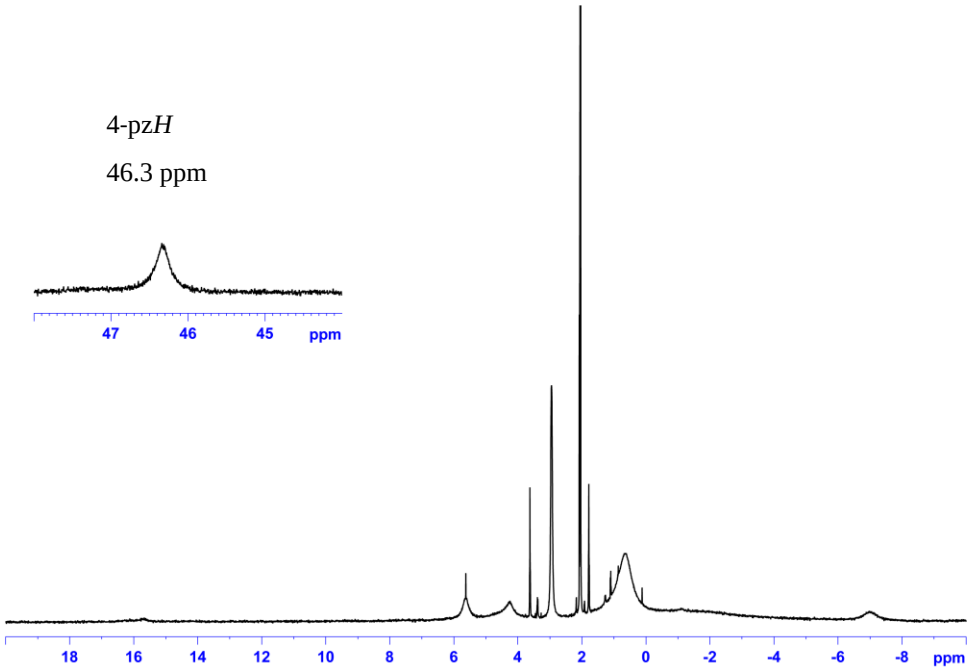

Figure S17. ^{1}H-NMR spectrum of [Co(κ^2-O_2N)$_2$(L1")] in $(CD_3)_2CO$ at room temperature.

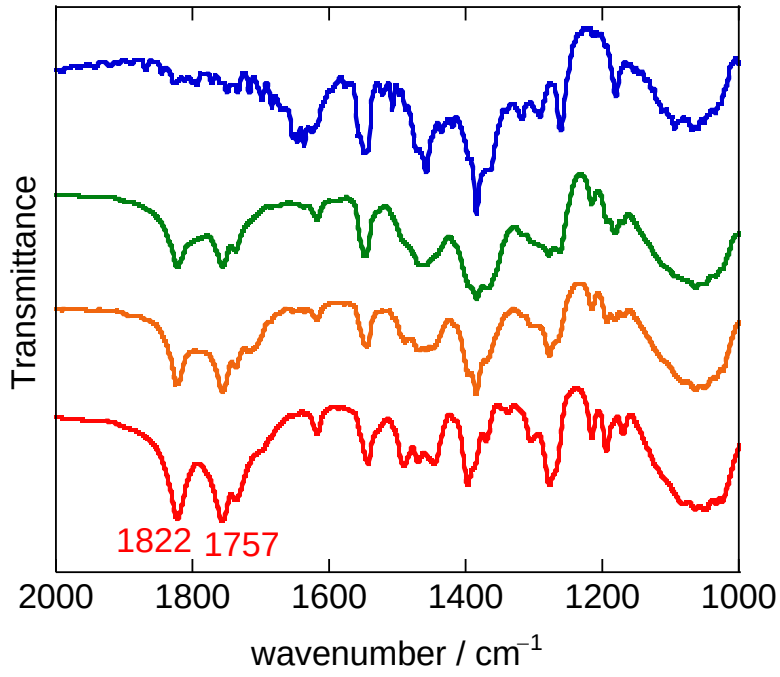

Figure S18. IR spectral changes of [Fe$(NO)_2$(L1")](BF_4) under argon atmospheres at room temperature (KBr) (red: start, orange: one week after, green: two weeks after, blue: three weeks after).

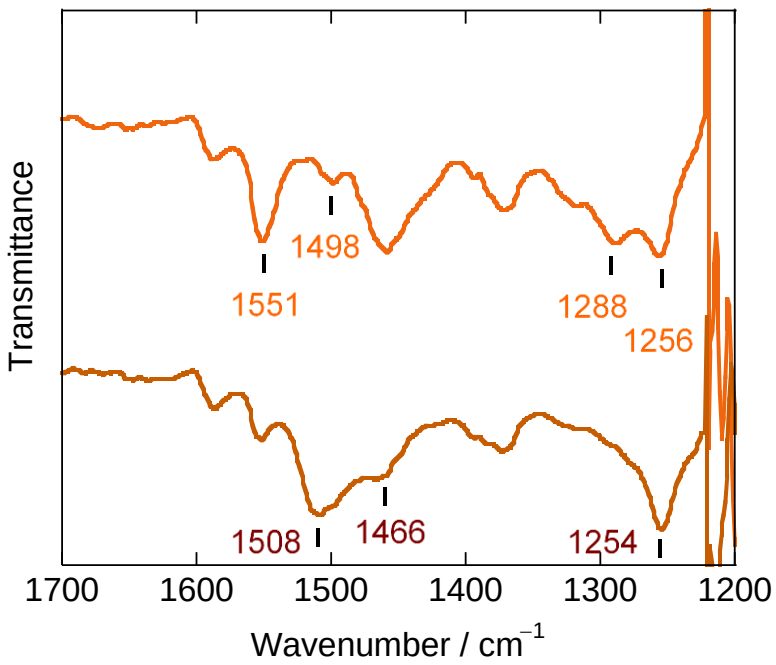

Figure S19. IR spectral changes during the O_2 reaction of $[Fe(NO)_2(L1")](BF_4)$ in solution (RT, CH_2Br_2). (top: normal NO and bottom: isotope labelled).

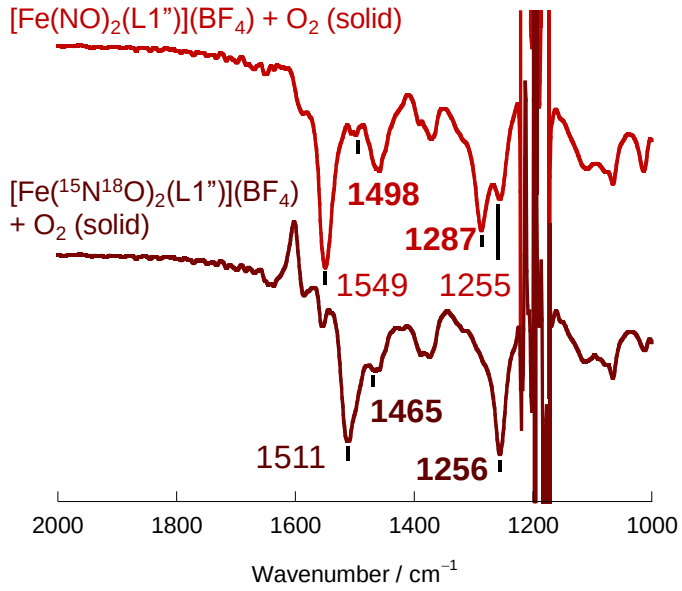

Figure S20. IR spectral changes during the O_2 reaction of $[Fe(NO)_2(L1")](BF_4)$ in the solid (RT, CH_2Br_2). (top: normal NO and bottom: isotope labelled).

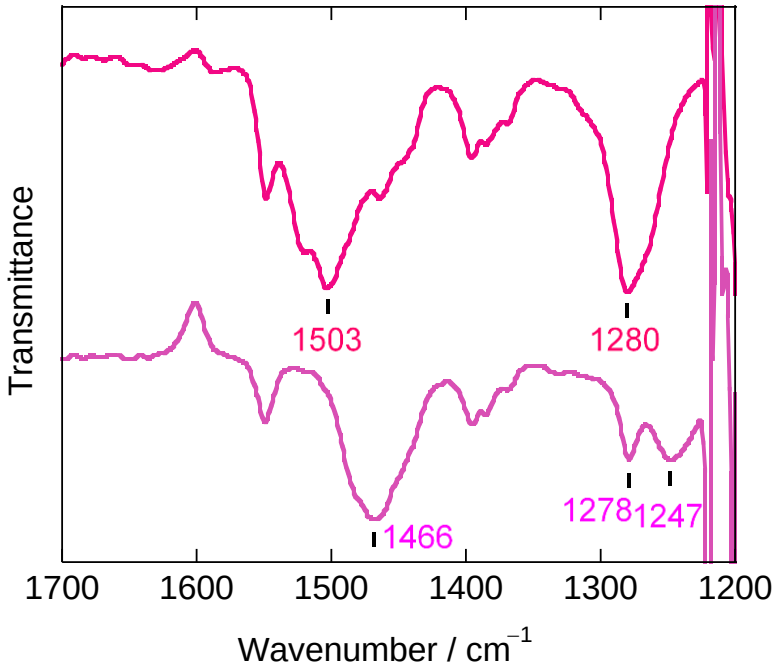

Figure 21. IR spectral changes during the dioxygen reaction of $[Co(NO)_2(L1'')](BF_4)$ in solution (RT, CH_2Br_2). (top: normal NO and bottom: isotope labelled).

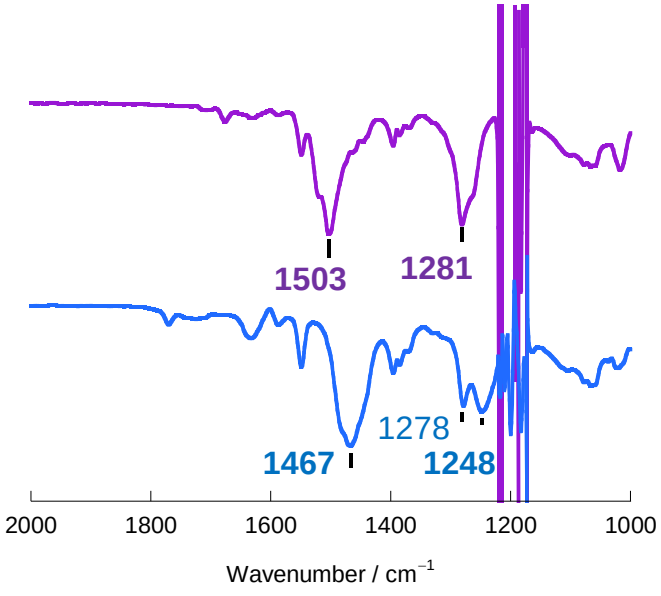

Figure S22. IR spectral changes during the O_2 reaction of $[Co(NO)_2(L1'')](BF_4)$ in the solid (RT, CH_2Br_2). (top: normal NO and bottom: isotope labelled).

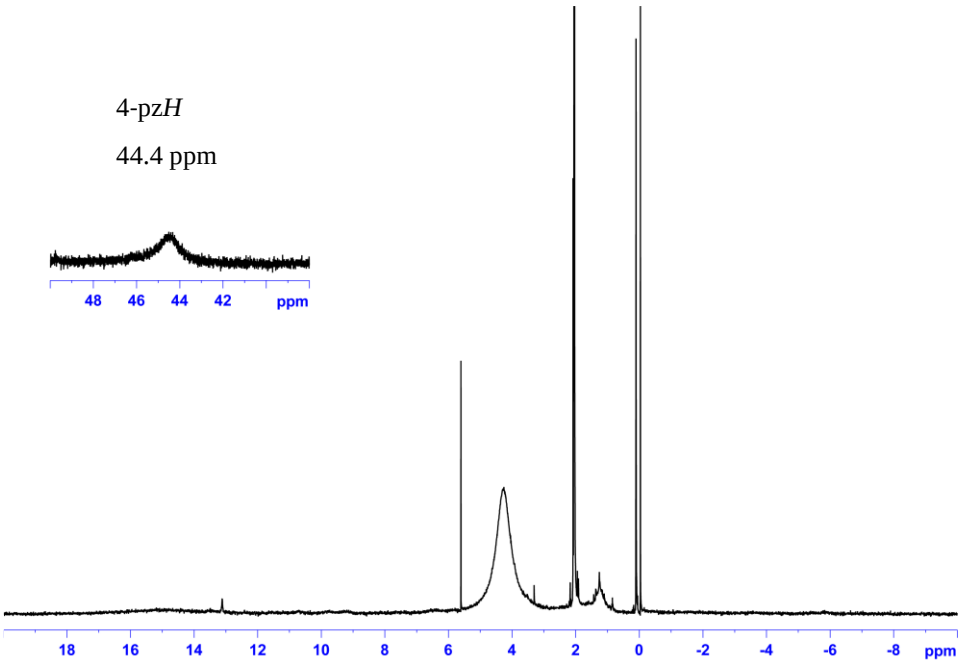

Figure S23. ^{1}H-NMR spectrum of the products of the O_2 reaction of $[Co(NO)_2(L1'')](BF_4)$ in solution. Taken in $(CD_3)_2CO$ at room temperature.

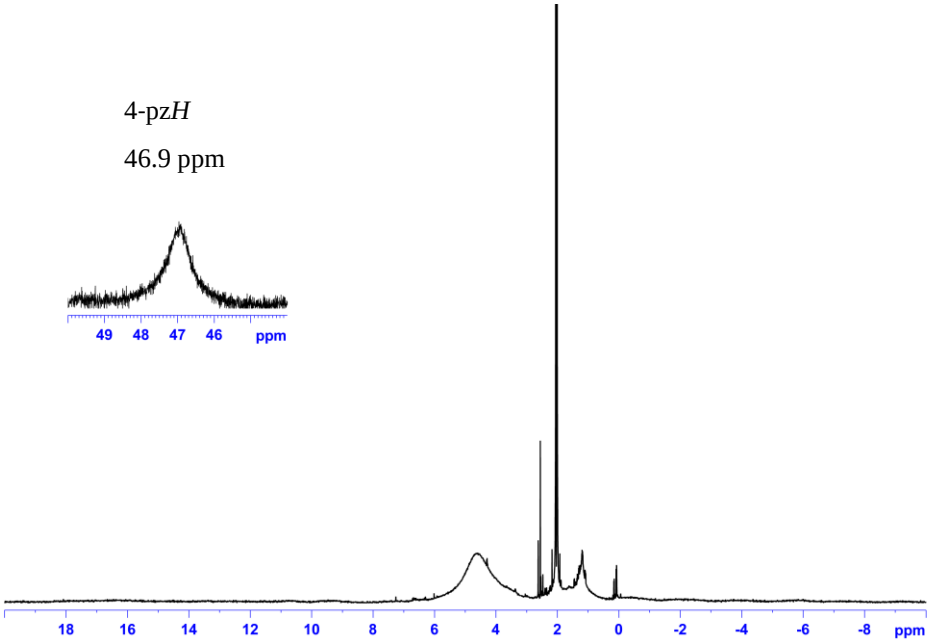

Figure S24. ^{1}H-NMR spectrum of the products of the O_2 reaction of $[Co(NO)_2(L1'')](BF_4)$ in the solid. Taken in $(CD_3)_2CO$ at room temperature.